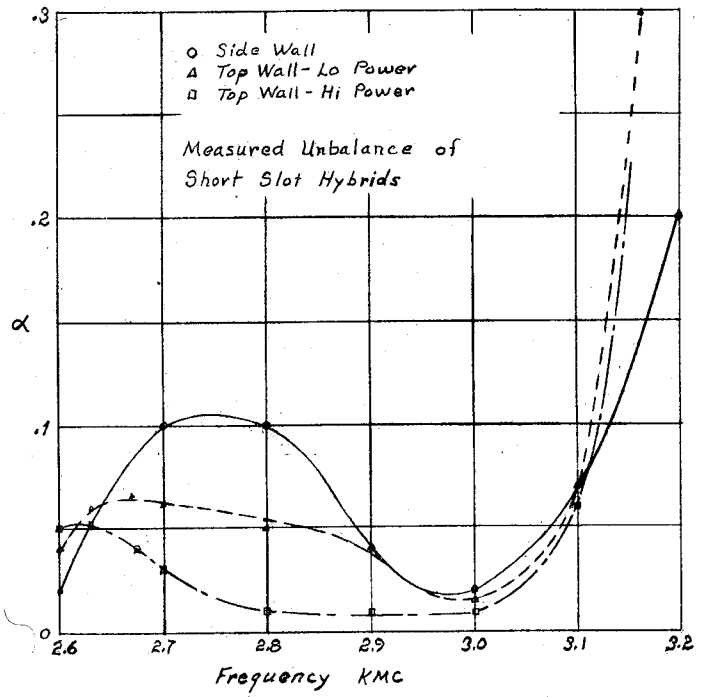

Fig. 10

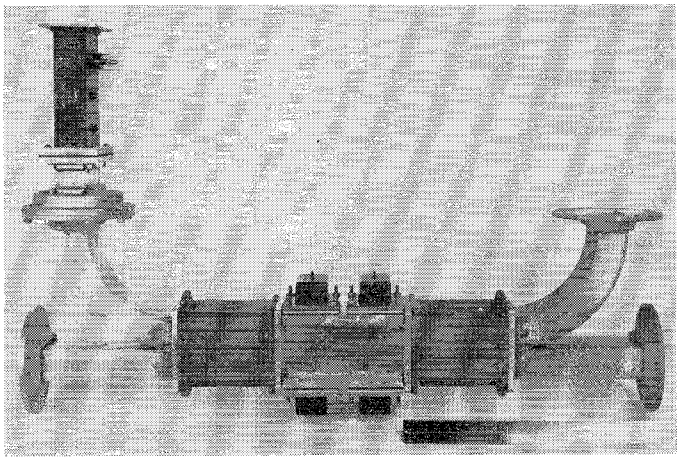

Fig. 11

considered only as a qualitative indication of the power handling ability.

The second duplexer, employing two-tube arrays in the switching circuit, behaved in a similar fashion at high level and had the predicted receiving bandwidth. This duplexer is shown in Fig. 11 (above).

Calculation of the Parameters of Ridge Waveguides*

TSUNG-SHAN CHEN†

Summary—**In this paper an algebraic expression which constitutes an approximation to Cohn's transcendental equation is given for the determination of the dominant-mode cutoff wavelength of ridge waveguides. A modified derivation of Mihran's equation for calculating the characteristic impedance of ridge waveguides is discussed. Based upon these formulas, nomographs are constructed to permit the determination of these parameters with sufficient accuracy when the waveguide and the ridge dimensions vary. Experimental verification of the calculated cutoff wavelength is included.**

Introduction

RIDGE WAVEGUIDES have a longer cutoff wavelength and a lower characteristic impedance than conventional rectangular waveguides having the same internal dimensions. The ridge waveguides also have a wider bandwidth free from higher-mode interference. Because of these advantages, ridge waveguides have been used as transmission links in systems requiring a wide free range in the fundamental mode,[1] as matching or transition elements in waveguide-to-coaxial junctions,[2] as filter elements, and as components for other special purposes.[3] One type of slow-wave structure used with traveling-wave tubes consists of a ridge waveguide which is made periodic by means of equally spaced transverse slots. The transverse resonant frequency of this structure corresponds to the cutoff frequency of the ridge waveguide.[4]

In the development of tunable magnetrons, double-ridge waveguides have been used as external tuning cavities because their reduced cutoff frequency permits a compact cavity section. Because the electric field is concentrated between the ridges, satisfactory tuning characteristics are obtained by means of a plunger which short-circuits the narrow gap. In the electron-beam method of frequency modulation, the beam is introduced in this region of strong electric field between two parallel plates attached to the ridges.

* Manuscript received by PGMTT, March 14, 1956.
† Radio Corp. of America, Harrison, N. J.

[1] T. N. Anderson, "Double-ridge waveguide for commercial airlines weather radar installation," IRE TRANS., vol. MTT-3, pp. 2–9; July, 1955.

[2] Radio Res. Lab. Staff, Harvard Univ., "Very High-Frequency Techniques," vol. II, pp. 678–684, 731–736, McGraw-Hill Book Co., Inc., New York, N. Y.; 1947.

[3] S. B. Cohn, "Properties of ridge waveguides," PROC. IRE, vol. 35, pp. 783–788; August, 1947.

[4] J. R. Pierce, "Traveling-Wave Tubes," D. Van Nostrand Co., New York, N. Y., ch. 4; 1950.

Ridge waveguides are also used as H-type output transformers in magnetrons for the purpose of transforming the high impedance of the waveguide used for power transmission to the low impedance level of the magnetron. If a rectangular waveguide transformer is employed, the dimensions required for impedance matching may be too large, especially for magnetrons having short block heights. When the H-type transformer is used, an effectively large width can be obtained with small physical sizes. In addition, good broadband characteristics may be provided by proper selection of the dimensions of the H section to yield a cutoff wavelength at least as long as that of the waveguide connected to the transformers.

In these applications of ridge waveguides, the cutoff wavelength and the characteristic impedance are important parameters to be known for design purposes, and approximate relations for their determination have been available.[5–7] Cohn[3] first developed the accurate transcendental expressions for cutoff wavelengths of odd and even TE_{mo} modes and also expressions for the attenuation and characteristic impedance of the TE_{10} mode. Recently Cohn's work has been extended to include unusual ridge dimensions and cross sections other than rectangular.[8–10] In this article, emphasis is laid upon the calculation of the dominant mode characteristics of rectangular ridge waveguides. Formulas for finding these characteristics are expressed explicitly in terms of the guide dimensions, and charts are constructed to facilitate computations for waveguides having various aspect ratios and having ridges of different widths and depths.

Cutoff Wavelengths for the Dominant Mode in Ridge Waveguides

Cross sections of single-ridge and double-ridge waveguides are shown in Fig. 1. In the derivations, mks units are used unless otherwise mentioned. In Fig. 2, a unit length of ridge waveguide is represented by a lumped-constant equivalent circuit consisting of capacitance and inductance in parallel. The capacitance, C, in the equivalent circuit consists of the electrostatic capacitance, C_s, and the discontinuity capacitance, C_d. When a single-ridge waveguide such as that shown in Fig. 1(a) is operating in the dominant mode, the capacitance, C_s, depends mainly on the region between the ridge and

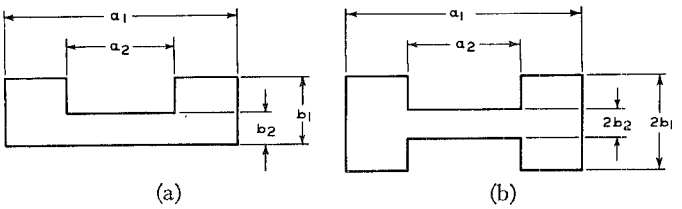

Fig. 1—Cross sectional view of (a) single-ridge and (b) double-ridge waveguides.

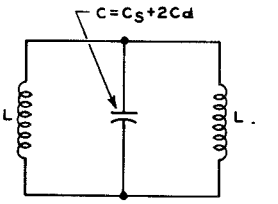

Fig. 2—Equivalent lumped-constant circuit for a unit length of ridge waveguide at cutoff wavelength.

the bottom plate, where a strong electric field exists This capacitance in farads per unit length of the guide is approximately given by

$$C_s = \frac{\epsilon a_2}{b_2} \tag{1}$$

where ϵ is the permittivity of the medium and in free-space equals 8.854×10^{-12} farad per meter.

The ridge in the waveguide presents discontinuities to the electromagnetic waves and causes local or higher-order waves. The effects of these local fields are included in the calculation by the addition at the proper location of the discontinuity susceptance which is here capacitive in nature. By the use of Hahn's method[11] of field matching, Whinnery and Jamieson[12] developed a series for the discontinuity capacitance, C_d, which depends on the step ratio, b_2/b_1, and, to a lesser extent, on the ratio a_2/b_2. The capacitance C_d along with the quantity $2C_d/\epsilon$ is plotted in Fig. 3 as a function of the step ratio b_2/b_1.

This discontinuity capacitance approaches closely the fringing capacitance in a constricted conductor, which is obtained by means of Schwarz-Christoffel transformation[12,13]

$$C_d = \frac{\epsilon}{\pi}\left[\frac{x^2+1}{x}\cosh^{-1}\left(\frac{1+x^2}{1-x^2}\right) - 2\ln\frac{4x}{1-x^2}\right] \tag{2}$$

where $x = b_2/b_1$. The value of C_d found from (2) can be shown to agree with that given by Fig. 3. The total capacitance C in farads per unit length of the waveguide is then

$$C = \frac{\epsilon a_2}{b_2} + 2C_d. \tag{3}$$

[5] G. B. Collins, ed., "Microwave Magnetrons," M.I.T. Rad. Lab. Ser., McGraw-Hill Book Co., Inc., New York, N. Y., vol. 6, pp. 198–203; 1948.

[6] G. L. Ragan, ed., "Microwave Transmission Circuits," M.I.T. Rad. Lab. Ser., McGraw-Hill Book Co., Inc., New York, N. Y., vol. 9, p. 57; 1948.

[7] S. Ramo and J. R. Whinnery, "Fields and Waves in Modern Radio," John Wiley and Sons, Inc., New York, N. Y.; 1944.

[8] Hans-Georg Unger, "Die Berechnung von Steghohlleitern," *Archiv Elekt. Ubertragung*, Band 9, Heft 4; April, 1955.

[9] J. M. Osepchuk, "Variational Calculations on Ridge Waveguides," Cruft Lab., Harvard Univ., Cambridge, Mass., Tech. Rep. No. 224; May 5, 1955.

[10] S. Hopfer, "The design of ridged waveguides," IRE Trans., vol. MTT-3, pp. 20–29; October, 1955.

[11] W. C. Hahn, "A new method for the calculation of cavity resonators," *J. Appl. Phys.*, vol. 12, pp. 62–68; January, 1941.

[12] J. R. Whinnery and H. W. Jamieson, "Equivalent circuits of discontinuities in transmission lines," Proc. IRE, vol. 32, pp. 98–116; February, 1944.

[13] Miles Walker, "Conjugate Functions for Engineers," Oxford University Press, Cambridge, Mass.; 1933.

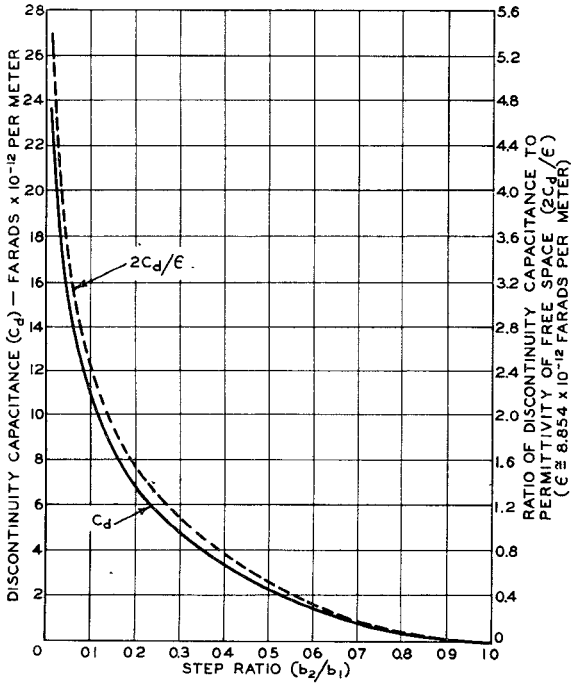

Fig. 3—Discontinuity capacitance, C_d, and the ratio, $2C_d/\epsilon$ as functions of the step ratio, b_2/b_1.

The inductances in the equivalent circuit show in Fig. 2 are determined by the sections of the waveguide on both sides of the ridge as shown in Fig. 1(a). The inductance, L, in henries due to either section per unit length of waveguide is given by

$$L = \frac{\mu(a_1 - a_2)}{2}(b_1), \tag{4}$$

where μ is the permittivity of the medium and equals $4\pi \times 10^{-7}$ henry per meter for free space. For the double-ridge waveguide depicted in Fig. 1(b), the capacitance C in (3) should be halved, and the inductance L in (4) doubled; the cutoff frequency remains unchanged.

At cutoff, the waves travel back and forth in the ridge waveguide in the transverse direction without longitudinal propagation; this condition corresponds to anti-resonance in the circuit shown in Fig. 2. The cutoff frequency, f_c', of the ridge waveguide in cycles per second is

$$f_c' = \frac{1}{2\pi\sqrt{(L/2)C}} \tag{5}$$

which, in conjunction with (3) and (4), becomes

$$f_c' = \frac{1}{\pi\sqrt{\mu\epsilon}\sqrt{\left(\frac{a_2}{b_2} + \frac{2C_d}{\epsilon}\right)(a_1 - a_2)(b_1)}}. \tag{6}$$

The cutoff wavelength, λ_c', of the ridge waveguide is given by $\lambda_c' = 1/(f_c'\sqrt{\mu\epsilon})$ and the cutoff wavelength λ_c of rectangular waveguide of width a_1 by $\lambda_c = 2a_1$. The ratio of these two cutoff wavelengths is

$$\frac{\lambda_c'}{\lambda_c} = \frac{\pi}{2}\sqrt{\left(\frac{a_2}{b_2} + \frac{2C_d}{\epsilon}\right)\left(\frac{b_1}{a_1}\right)\left(1 - \frac{a_2}{a_1}\right)}. \tag{7}$$

A nomograph for the determination of λ_c'/λ_c for ridge waveguides having known dimensions is shown in Fig. 4 (opposite). The value of $2C_d/\epsilon$ corresponding to a given step ratio, b_2/b_1, is found from Fig. 3. A line joining this value and the given point on the a_2/b_2 scales determines the sum $(a_2/b_2 + 2C_d/\epsilon)$. A second line is then drawn connecting the two given points a_1/b_1 and a_2/a_1 on the horizontal scales and cutting the diagonal at a definite point. A final line from the point $(a_2/b_2 + 2C_d/\epsilon)$ through this intersection determines the value of λ_c'/λ_c on the right-hand scale.

Cutoff Wavelengths for the Higher Modes in Ridge Waveguides

To find the cutoff wavelengths of higher modes, the single-ridge waveguide shown in Fig. 1(a) is considered as a composite transmission-line system having waves traveling in the transverse direction.[3] In Fig. 5(a), one half of a length, d, of the guide is represented by two sets of parallel plates separated by distances b_1 and b_2. The odd mode of the TE_{mo} wave requires a voltage loop and a current node at the center of the waveguide; the equivalent circuit shown in Fig. 5(b) should have an open circuit at the left end and a short circuit at the right end. In this circuit,

$\theta_1 = \left(1 - \frac{a_2}{a_1}\right)\frac{\lambda_c}{\lambda_c'}\frac{\pi}{2} =$ electrical length of section X_1 in radians.

$\theta_2 = \frac{a_2}{a_1}\frac{\lambda_c}{\lambda_c'}\frac{\pi}{2} =$ electrical length of section X_2 in radians.

$Y_{01} = \sqrt{\frac{\epsilon}{\mu}}\left(\frac{d}{b_1}\right) =$ characteristic admittance of section X_1 in mhos.

$Y_{02} = \sqrt{\frac{\epsilon}{\mu}}\left(\frac{d}{b_2}\right) =$ characteristic admittance of section X_2 in mhos.

$B_c' = 2\pi f_c' dC_d =$ discontinuity susceptance for a length d of the composite line in mhos.

The cutoff condition of the waveguide corresponds to resonance of the equivalent circuit,[3,10,14] which leads to an expression giving the cutoff wavelength, λ_c', implicitly in terms of the guide dimensions

$$\frac{b_1}{b_2} = \frac{\cot\left[\left(1 - \frac{a_2}{a_1}\right)\frac{\lambda_c}{\lambda_c'}\frac{\pi}{2}\right] - \frac{2C_d}{\epsilon}\frac{b_1}{a_1}\frac{\lambda_c}{\lambda_c'}\frac{\pi}{2}}{\tan\left(\frac{a_2}{a_1}\frac{\lambda_c}{\lambda_c'}\frac{\pi}{2}\right)}. \tag{8}$$

This equation is solved for the first order root to obtain the cutoff wavelength of the TE_{10} mode and for higher-

[14] N. Marcuvitz, "Waveguide Handbook," M.I.T. Rad. Lab. Ser., McGraw-Hill Book Co., Inc., New York, N. Y., vol. 10, pp. 399–402; 1951.

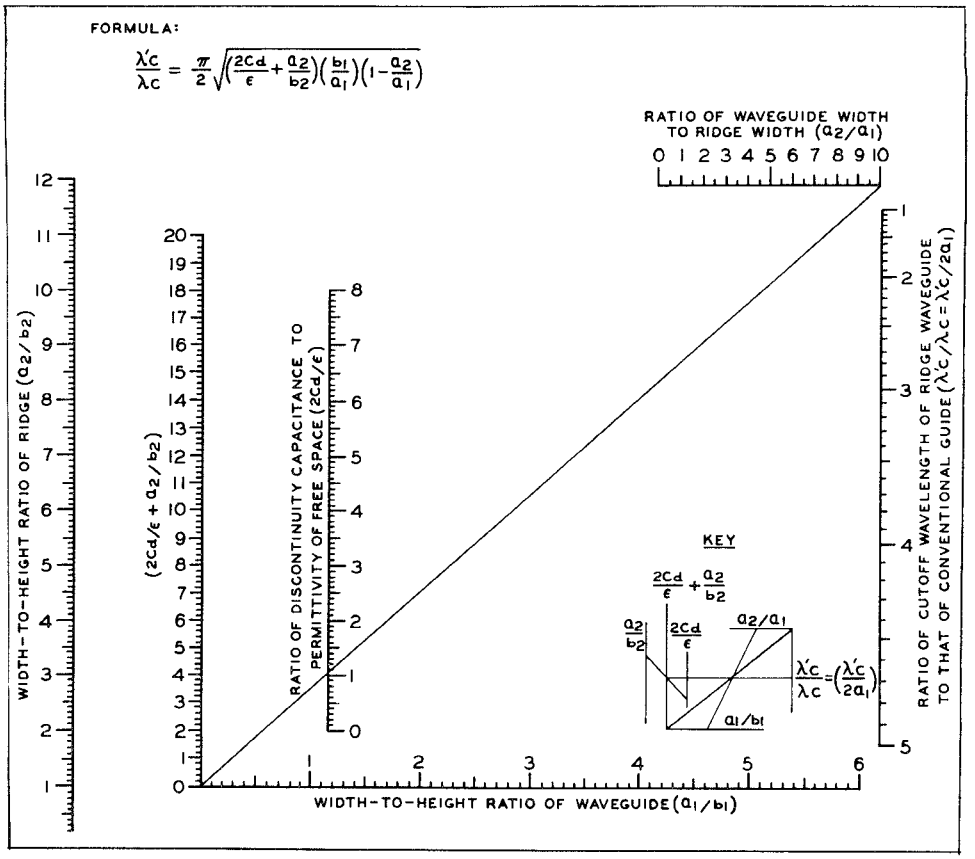

Fig. 4—Nomograph for the determination of the ratio, λ_c'/λ_c, of the cutoff wavelength, λ_c', of a ridge waveguide to the cutoff wavelength, λ_c, of a conventional rectangular waveguide having the same internal dimensions.

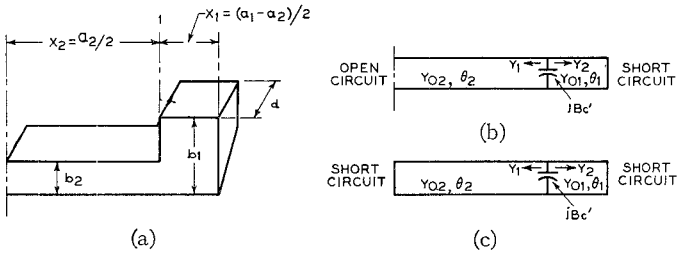

Fig. 5—Equivalent distributed parameter circuits for one half of a unit length of (a) ridge waveguide, (b) for odd modes of TE_{mo} waves, and (c) for even modes.

order roots to obtain the cutoff wavelengths of the higher-order odd TE_{mo} modes.

Because the ratios appearing in the arguments of the trigonometric functions are substantially less than unity, these functions can be replaced by the first two terms of their series expansions. Eq. (8) then becomes

$$\left[\frac{b_1}{b_2}\left(\theta_2 + \frac{1}{3}\theta_2^3\right) + \frac{2C_d}{\epsilon}\frac{b_1}{a_2}\theta_2\right] \cdot \left[\left(\frac{a_1}{a_2} - 1\right)\theta_2 + \frac{1}{3}\left(\frac{a_1}{a_2} - 1\right)^3\theta_2^3\right] = 1. \quad (9)$$

When the cubic terms in (9) are discarded and remaining terms are solved for λ_c'/λ_c, (7) is obtained.

To improve the accuracy of λ_c'/λ_c determined from the chart, this approximate value is substituted only in the cubic terms of (9); the result is a quadratic equation θ_2 or in λ_c/λ_c'. This equation can be solved readily to obtain a more accurate value of λ_c'/λ_c.

The even modes of the TE_{mo} waves have voltage nodes at the center and at the end of the waveguide section in Fig. 5(a); the equivalent circuit for these modes becomes Fig. 5(c). The cutoff wavelengths of the TE_{20} and higher-order even modes as determined by the resonance of this circuit are given by

$$\frac{b_1}{b_2} = \frac{\frac{2C_d}{\epsilon}\frac{b_1}{a_1}\frac{\lambda_c}{\lambda_c'}\frac{\pi}{2} - \cot\left[\left(1 - \frac{a_2}{a_1}\right)\frac{\lambda_c}{\lambda_c'}\frac{\pi}{2}\right]}{\cot\left(\frac{a_2}{a_1}\frac{\lambda_c}{\lambda_c'}\frac{\pi}{2}\right)}. \quad (10)$$

Characteristic Impedance of Ridge Waveguide

The characteristic impedance of ridge waveguide derived on the voltage-to-current basis is used in the calculation of tuning curves for a magnetron which is tuned by means of a ridge cavity attached to one of the magnetron resonators. This parameter is also used in impedance-matching problems. In the formulation of the voltage-to-current ratio, the current is separated into two components: 1) a longitudinal component on the top and bottom plates of the waveguide, which excites the principal fields, and 2) another longitudinal component at the point where the waveguide height changes, which produces the local fields.

The first component of current, I_{z1}, is determined by the field distribution along the waveguide cross section as shown in Fig. 6(a) and 6(b). Cohn[3] derived the expression for I_{z1} as

$$I_{Z1} = \frac{1}{Z_{TE}}\left(\frac{V_0}{b_2}\right)\left(\frac{\lambda_c'}{\pi}\right)\left(\sin\theta_2 + \frac{b_2}{b_1}\cos\theta_2 \tan\frac{\theta_1}{2}\right) \quad (11)$$

where:

V_0 = the amplitude of voltage distribution at the center of the waveguide cross section

$$Z_{TE} = \frac{\sqrt{\frac{\mu}{\epsilon}}}{\sqrt{1-\left(\frac{\lambda}{\lambda_c'}\right)^2}} = \text{characteristic wave impedance.}$$

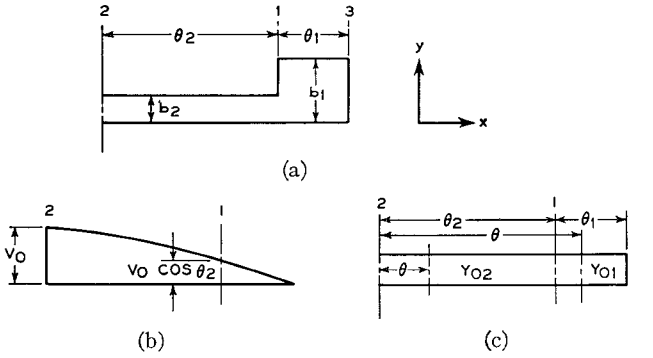

Fig. 6—(a) Cross section of ridge waveguide; (b) curve of voltage distribution across (a); (c) equivalent transmission line circuit.

Because the value of capacitance given by (2) agrees very closely with that found by the process of matching fields, the second current component, I_{z2}, can be determined from a consideration of the electrostatic field existing in the discontinuity region. Fig. 7 shows the field distribution at the ridge corner of a unit length of waveguide. In the derivation that follows, W represents the width of the region over which the local fields are predominant, Q the total charge over the same region, and E the electric field intensity at the discontinuity. The potential at plane 1 in Fig. 6(c) is given by

$$V_1 = V_0 \cos\theta_2$$

and by the use of Gauss' law

$$\epsilon E(W)(1) = Q = C_d V_1 = C_d V_0 \cos\theta_2,$$

from which

$$E = \frac{C_d V_0 \cos\theta_2}{\epsilon W}.$$

The magnetic field strength, H, in ampere-turns per meter is given by $H = E/Z_{TE}$ and the longitudinal current for both sides of the ridge by

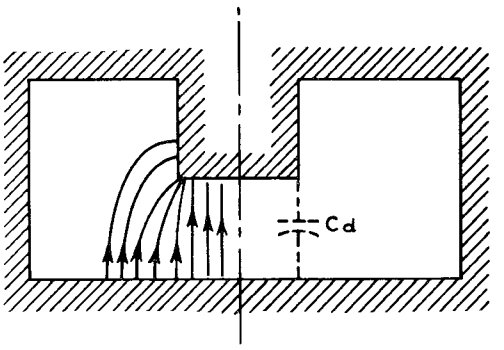

Fig. 7—Electrostatic-field distribution at corner of unit length of ridge waveguide.

$$I_{Z2} = 2HW = \frac{2C_d V_0 \cos\theta_2}{\epsilon Z_{TE}}. \quad (12)$$

Eq. (12) agrees with Mihran's result.[15]

The characteristic impedance, Z_0, of the ridge waveguide is then

$$Z_0 = \frac{V_0}{(I_{Z1} + I_{Z2})} = \frac{Z_{0\infty}}{\sqrt{\left(1-\frac{f_c'}{f}\right)^2}}, \quad (13)$$

where

$$Z_{0\infty} = \frac{\sqrt{\frac{\mu}{\epsilon}}}{\frac{2C_d}{\epsilon}\cos\theta_2 + \frac{1}{\pi}\frac{\lambda_c'}{b_2}\left(\sin\theta_2 + \frac{b_2}{b_1}\cos\theta_2\tan\frac{\theta_1}{2}\right)}. \quad (14)$$

Because the ratios λ_c/λ_c' and a_2/a_1 are considerably less than unity for narrow ridges, $\cos\theta_2$ is approximately equal to 1, $\sin\theta_2$ to θ_2, and $\tan\theta_1/2$ to $\theta_1/2$. If the medium is free space and θ_2 and $\theta_1/2$ are less than 20°, (14) can be approximated by

$$Z_{0\infty} = \frac{120\pi}{\frac{2C_d}{\epsilon} + \frac{a_2}{b_2} + \frac{1}{2}\frac{a_1}{b_1}\left(1-\frac{a_2}{a_1}\right)^2}. \quad (15)$$

Based upon (15) and (13) the nomograph in Fig. 8 is constructed for the determination of $Z_{0\infty}$ and Z_0. For double-ridge waveguides, the value of Z_0 found from the left-hand side of the chart should be multiplied by 2.

Experimental Verification

In the development of a 10-kilowatt, 825-megacycle magnetron, a double-ridge waveguide was coupled to the magnetron to maintain a constant center frequency. The dimensions of the double-ridge cavity in centimeters were as follows: $a_1 = 16$, $a_2 = 2.56$, $2b_1 = 25.6$, and $2b_2 = 6$. Eqs. (7) and (9) are used to obtain $\lambda_c' = 2.095\,\lambda_c$ where $\lambda_c = 32$ centimeters. The guide wavelength, λ_g, is

[15] T. G. Mihran, "Closed- and open-ridge waveguides," Proc. IRE, vol. 37, pp. 640–644; June, 1949.

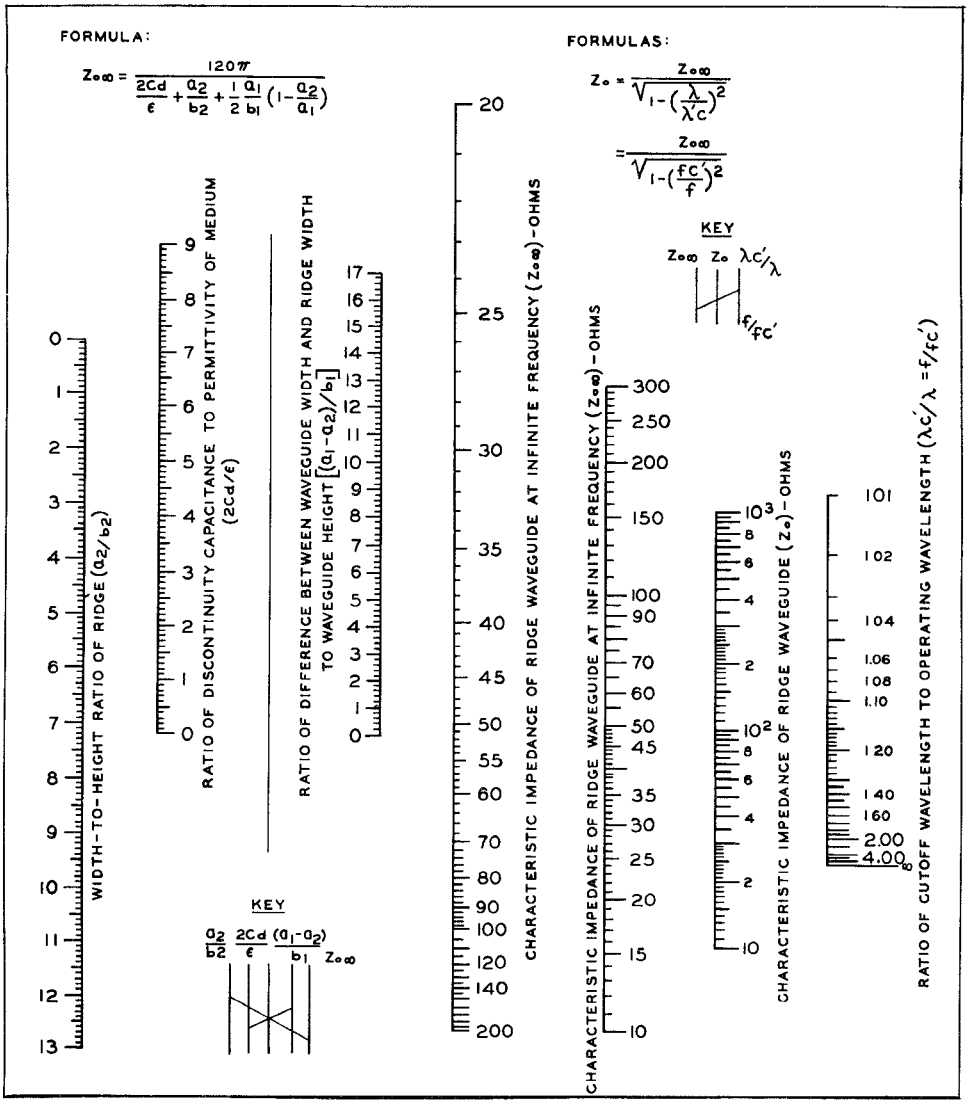

Fig. 8—Nomograph for determination of characteristic impedance of ridge waveguides having narrow ridges.

calculated from the relation

$$\lambda_g = \frac{\lambda}{\sqrt{1-\left(\frac{\lambda}{\lambda_c'}\right)}}$$

in which λ is the free-space wavelength corresponding to a particular frequency. At the resonant frequency, the cavity length should be half the guide wavelength of the ridge waveguide. For wavelengths of 40 and 30 centimeters, the calculated values of $\lambda_g/2$ as shown in Fig. 9 were 9.7 and 6.6 inches as compared with the measured values of 9.6 and 6.6 inches, respectively.

The characteristic impedance obtained from (15) and (13) was used to check the cold resonant frequency of the magnetron-cavity combination as a function of the cavity length. The measured and calculated results were in close agreement.

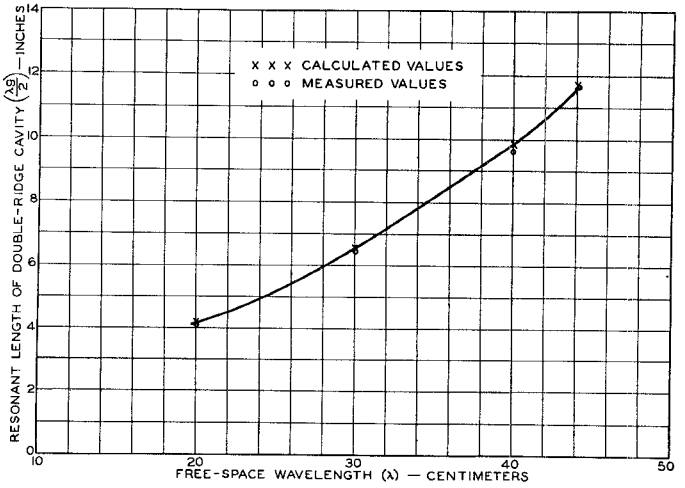

Fig. 9—Tuning curve for double-ridge cavity to be coupled to 10-kilowatt, 825-megacycle developmental tunable magnetron.